Proceedings of the Korean Nuclear Society Autumn Meeting
Hanyang Univ., Seoul, Korea, Oct. 30 - 31 1998

Neutron Irradiation Effects on the Microstructural Dependence of Mechanical Properties of SA 508 Cl. 3 RPV Steels

Se-Hwan Chi[1], Milan Brumovsky[2]

1. Korea Atomic Energy Research Institute
P.O Box 105, Yusong, Taejon, 305-600 Korea
2. Nuclear Research Institute Rez plc 250 68 Rez Czech Republic

Abstract

Differences in the neutron-induced mechanical property change for four kinds of reactor pressure vessel (RPV) steels of different manufacturing process were investigated based on the differences in the unirradiated microstructure. Microvickers hardness, indentation, and miniature tensile specimen tests were conducted for mechanical property measurement and optical microscope (OM) and transmission electron microscope(TEM) were performed for microstructural characterization. Specimens were irradiated to a neutron fluence of 2.7 x 10^{19}n/cm^2 (E$\geq$ 1 MeV) at 288℃. Investigation on the unirradiated microstructures showed largely the same microstructure in that tempered acicular bainite and ferrite with bainitic phase are prevailing. Noticiable differences were observed in the grain size and distribution of cementite, and bainitic lath microstructures. No noticiable changes were observed in the optical and thin film TEM microstructures after irradiation. Apparent differences, however, were observed in the results of mechanical testing after irradiation. Results of tensile testing and hardness measurement show that the present steel refined by vacuum carbon deoxidation(VCD) method exhibits exceptionally high radiation hardening behavior among the four kinds of steel of similar chemical composition examined in the present study. This observation implies that the current irradiation embrittlement prediction method based only on the major alloying elements and fluence could yield nonconservative prediction for this steel. The present results strongly suggest that a new material-specific embrittlement prediction method that considers the differences in the unirradiated microstructural state should be developed and applied .

I. Introduction

Even the current RPV embrittlement prediction method is based on the accumulation of surveillance data from a lot of commercial power reactors of different RPV steels, we still can not fully rule out a possibility that extraordinary RPV steels which are out of the boundary of the database used for Reg. Guide 1.99(Rev. 2) may be produced. The possibility of extraordinary RPV steels can be assumed when the current understanding of RPV embrittlement is considered microstructurally. The current code prediction do not provide any method that regulates the steels whose microstructure is quite different even the chemistry reside in the boundary. It is generally agreed that in most instances the embrittlement phenomena is the direct result of hardening due to the development of a fine-scale damage microstructure induced or enhanced by irradiation. So, it is expected that any microstructural variables that affect the hardening of the RPV steels in the unirradiated condition will also influence the hardening of the irradiated material.

In the present work, recognizing the importance of microstructural states to embrittlement, the microstructural dependence of irradiation-induced hardening in the four kinds of RPV steels of different initial microstructure was investigated.

II. Experimental

II.1 Materials and specimen preparation.

Coupons used for specimen preparation were extracted from four shell forgings which differed in the steel refining process. Chemical composition and the employed steel refining process of the materials are summarized in **Table 1** and the heat treatment conditions of the shell forgings are summarized in **Table 2.** Schematics of each shell forging manufacturing processes are quite similar each other except the major steel refining processes. Coupons, and specimens were machined and prepared from 1/4 T (thickness) locations of the shell forgings. Miniaturized tensile specimens in the size of 27.5 X 5.0 X 0.5 mm(gage length: 9 mm) were used in the present study. Vickers microhardness tests were performed on hardness disc specimens machined from each coupons.

II.2 Irradiation.

Prepared specimens were irradiated to the neutron fluence of about 2.7 x 10^{19} n/cm^2 (E≥1 MeV) at LVR-15 experimental reactor in the NRI(nuclear research institut) Rez, Czech Republic using a rig CHOUCA MT. Specimens were kept in inert atmosphere(He, Ar) at the pressure of 80 - 140 kPa during irradiation. Six kinds of fluence monitors, i.e., Ti, Cu, Ni, Fe, Nb, and Co, were used at nine locations in the specimen carrier. Irradiation temperature was controlled by six heaters of the rig and twelve thermocouples type K with measuring junction insulated, 1 mm in diameter, six of them being placed just on the heaters middle position, were installed for irradiation temperature measurement. Except the stainless steel nut, all other components of carrier were made of aluminum or aluminum-magnesium alloy(Al-Mg_5). Neutron flux and irradiation temperature were about 2.7 x 10^{13} n/cm^2. sec and 288 ± 10℃, respectively. It is worth to note that the fluence in the present study roughly corresponds to the design end life fluence of a reactor. The schematics of carrier used for the present irradiation. are reported elsewhere [4].

II.3 Microstructural investigation.

For optical microscopy, specimens in size of about 4 x 4 mm were polished to 0.3 ㎛ Al_2O_3 powder, etched in 1.5～3 % Nital for 10 ～ 20 sec, and examined in Nikon(EPIPHOT-THE) Inverted Microscope. The grain size was determined by the three-circle(or Abrams) procedure of ASTM E-112-88 at x 400. Investigation of microstructures and carbide morphology was performed by TEM(JEOL 2000FX). Disc specimens (3 mm Φ) were prepared by a submerged electrolytic jet thinning technique in a solutuion of 10% perchloric acid and 90% acetic acid at 30 to 35 V of applied voltage. To quantify possible differences in a detailed carbide size and density upon materials on TEM, carbon extraction replicas were prepared. The polished area of specimens were moderately etched with 4 % Nital for 60 ～ 120 sec to expose carbide clusters. Specimens were then mounted on a glass slide for carbon coating by vacuum evaporation in a Veeco high vacuum evaporation chamber. Evaporation of the sharpened rod required approximately 2 minutes at a 20 amp level. The specimen slide was rotated approximately 120^o under the evaporation source between each deposition to provide a uniform deposition thickness and prevent inconsistencies due to shadowing and fixture geometry. Carbon specimens were scored into about 2 x 2 mm^2. Stripping was performed in 10 % HCl + 90 % ethanol solution at about 0.1 ampare for about 4～5 minutes using a platinum wire as a cathode until the scored carbon peeled off. Cu grids of 400 mesh and 3 mm ∅ were then used to collect floating replicas. The replicas were then examined by TEM for precipitates morphologies, and were photographed for precipitates size and density determination .

II.4 Mechanical test.

Tensile tests were performed on an Instron 1122, 1,000 pound capacity, screw-driven load frame. Tests were conducted at ambient temperature at a constant displacement rate of 8.5 x 10^{-3}mm/sec. A special fixture was fabricated to facilitate loading specimens into grips without deforming the specimen. Load-displacement data were recorded on an X-Y recorder and , in addition, the data were digitized and recorded in a computer-based data bank. An average of 500 load-displacement points per specimen were saved. Vickers microhardness tests were performed on hardness disc specimens machined from each coupons. An automated Wilson Tukon microhardness tester was used to perform at least 10 indentations per specimens at room temperature. Load and duration were 300 g and 20 sec, respectively. Average DPH values with the standard deviation were automatically obtained from all of the indentation data by using a developed software. Details of the automated hardness tester are reported elsewhere [5].

III. Results.

III.1 Comparison of microstructure

TEM results on unirradiated and irradiated specimens are seen in **Fig. 1.** Comparisons of the grain size, precipitates and carbide morphology, precipitates number per unit area, and lath microstructure were made based on the OM and TEM results in the unirradiated condition, and summarized in **Table 3**. First of all, it is seen that all materials show largely the same bainitic microstructure in that tempered acicular bainite and ferrite with bainitic phase prevailing in the unirradiated condition irrespective of materials and no noticeable changes were observed in the thin film TEM microstructures after irradiation. This observation on irradiated microstructure of RPV steels already have previously been reported and discussed in detail by Buswell [6]. Band-shaped segregation were clearly observed for A, B, and C except D. As summarized in **Table 3**, there were some differences in grain size, especially between A and B, C, D. The grain size of A is 50% larger than the B, C and almost double that of D. It is well known that, for austenite grain size control using aluminum nitride particles [7], aluminum and nitrogen levels are controlled to achive austenite grain sizes in the range ASTM 7 - 10 (10 - 30 ㎛) [8]. Accordingly, the absence of aluminum addition in A versus B, C, D can account for the larger grain size. Round cementites and acicular Mo_2C carbides were found in all steels. No apparent difference was seen in the size of acicular Mo_2C carbides, which were mostly 50 - 100 nm. However, the size of the cementite particle in steel A was about 10 - 20 times larger than that of C and D. Moreover, large agglomerated islands of round cementites were frequently observed in A, but not in D. The size of the agglomerates in A, mostly larger that 30㎛ in length, were larger than the average grain size of A (～22㎛). Alloy C showed a larger carbide density than A and D for all three types of carbide morphology. For A and D, with roughly the same number density of carbides, the number of needle-like Mo_2C was a little higher in A than D. Recent results of Minfa Lin et al [9] show that the precipitation of needle-like carbides during tempering is related to the upper-nose temper embrittlement. The long square rod and round carbides in A appear to be precipitated along the lath boundary, but round and needle-like carbides appear to be precipitated along the grain boundary and inside of the lath, respectively. From the TEM results on thin films, it was observed that the lath boundary in A was not developed well compared to B, C, and D. D showed the narrowest lath width(2㎛) and A showed the widest(5㎛). Interlath carbides were found in A, B, and C and were thickest in A. A low cooling rate during quenching has been attributed to the growth of interlath carbides [10]. As remarked previously, even the complicated microstructural state of the heat treated bainitic steels prevents easy quantification of possible microstructural changes due to irradiation, it is seen that, at least under the present experimental conditions(OM, TEM), no observable changes were characterized after irradiation.

III.2 Tensile and Hardness Test.

Results of the tensile and Vickers microhardness tests on unirradiated and irradiated specimens are summarized in **Fig. 2** and **3**, respectively. Firstly, it is seen that the tensile strength(yield, ultimate tensile) has increased and ductility(uniform and total) has decreased with the increase in the hardness for all materials after irradiation. The changes in the strength was quite apparent compared to the elongation due to irradiation. Thus, the yield and tensile strength of these four materials have increased for about 5% - 19 %, but the uniform and total elongation decreased only for about 0.5% - 1.4%. In addition, it is seen in Fig. 2(I) that the differences in yield strength among materials have enlarged after irradiation. This observation strongly suggests that the degree of radiation sensitivity of each material is different to each other. It is also worth to note that the standard deviations of strength data(yield and tensile) in irradiation condition are quite big compared to those of elongation(uniform and total). This observation can partly be attributed to the possible large differences in the type and number density in irradiation-induced defects which are responsible for friction hardening after irradiation [11]. The deviation in the irradiated yield strength is the largest in the tensile parameters measured. Some of these observation may easily be understood through the comparisons of TEM thin film results on irradiated and unirradiated materials. Thus, no appreciable changes in the size, distribution, density, and morphologies of large carbides in the irradiation condition strongly imply that there should be no appreciable changes in the tensile properties after irradiation. However, the enlargement of the differences in the yield strength after irradiation strongly suggests that the degree of radiation sensitivity of each material is different to each other possibly due to the unidentified irradiation-induced defect microstructures . **Figs. 2(I)** and **2(IV)** show that A exhibits the largest increase in the yield strength and the largest decrease in the total elongation. Compared to A, D showed morderate increase in the strength but the least decrease in the uniform and total elongation, Fig. **2(III)** and **2(IV)**. This observation can also be assumed to be resulted partly from the differences in the carbide(cementite) size and distribution as compared in **Table 3**. Thus, compared to A, the narrowest banitic lath width, the smallest grain and cementite size, well developed lath boundary, well dispersed carbides through the matrix, and free of interlath carbides are assumed to have resulted in this observation. The fracture toughness as well as Charpy impact test data also have shown that D leads other materials [12].

Hardness data in **Fig. 3** show that the range of data distribution has increased after irradiation as in the case of yield strength data. It is seen that the increase in A is the largest and vice versa for D. The increase in A (37%) was almost double of D(19%). From the correlation between the yield strength and Vickers microhardness data, no apparent correlation trend was observed due to the scarcity in data.

IV. Discussion

As a whole the over-all sensitivity of the materials to neutron irradiation agrees well , within the scatter bound, with the previously reported results on commercial RPV steels except A [13]. However, the present results apparently show that A shows exceptionally higher sensitivity to irradiation than the other materials: As seen in the **Fig. 2(I)**, the rate of increase in the yield strength of A is about 1.8 - 3.4 times higher than those of C and D. In addition, this increase in A (19 % in crease) is well beyond the database(8 - 18 % increase) at about the same irradiation condition. It is worth to note that the increase in yield strength at room temperature is chosen as the most sensitive measure of irradiation [14]. Result of Vickers microharedness has also shown that the rate of increase of A to D was about 2. Material A showed also the largest decrease in total elongation measurements. Comparisons made with the previously reported results [15] also showed that, even for nearly the same fluence, irradiation temperature and chemistry, the yield strength of A appeared to increase about 10 MPa more than the other steels. Currently it is hard to explain clearly why only the material A shows the highest sensitivity to neutron irradiation among the materials of same microstructure and chemistry. As noted previously, microstructures revealed by OM and TEM explain well the inferior fracture-related elongation behavior in A as seen in **Fig. 2(III)** and **2(IV)**. Most of these observations in elongation may be attributed to the large grain size with the elongated and large, agglomerated carbides often encountered along the grain boundaries in A [16]. However, present results are insufficient and, in some sense, contradict to the highest hardening behavior of A. As seen in **Fig. 2(I)**, material A shows nearly the same yield strength with the other steels in the unirradiated condition. Thus, the differences between the steels are negligible in the unirradiated condition. This observation is quite reasonable in that all the compared RPV steels were commercially manufactured to the strict requirements of ASME materials code on RPV steel. The code specifies major factors(variables) affecting the mechanical properties of the RPV steels including the chemistry and heat treatment condition . **Fig. 1** also does not show any apparent modifications in microstructure after irradiation or any differences between the unirradiated and the irradiated condition . With only this observation and results, however, the amplified differences between the yield strength values and the highest hardening behavior of A after irradiation are difficult to explain. Part of these observation may be attributed to the extremely fine size(< 10 nm) of irradiation-induced defects which are not easily characterized by conventional TEM [17] and to the different steel refining processes employed [18]. For these irradiation-induced defects as in the case of low copper RPV steels of the present study, irradiation-induced increase in the yield strength, thus, radiation hardening, has recently been remarked by the formation of extremely fine nanovoid-complexes and interstitial loop-complexes as candidates with small phosphides, carbides and nitrides [19]. Further examinations using a wide array of sophistigated tools (for example, SANS, APFIM) are required to understand and fully characterize the extraordinary high radiation hardening behavior of A.

Here, it is worth to note that even the material A show the exceptionally highest hardening behavior in the steels of similar chemistry, little difference will be observed in the embrittlement prediction for these four materials since the current embrittlement prediction methods, including Reg. Guide (Rev. 2), consider only the content of Cu or Ni elements with neutron fluence. Thus, the prediction does not cosiders the apparent effects of microstructural differences in the steel of similar chemistry. In this regard, under the realization of the microstructural dependence of embrittlement, a new embrittlement prediction method that considers the microstructural differences seems to be developed and applied.

V. Conclusion

Differences in the irradiation-induced mechanical property change for four kinds of commercial RPV steels differing in microstructures partly due to different steel refining processes have been investigated. For nearly the same microstructures before and after irradiation, steel A refined by the vacuum carbon deoxidized process appeared to have the highest sensitivity to neutron irradiation. A showed the highest increase in yield strength and Vickers microhard-ness, and the largest decrease in total elongation. Part of these observation can be attributed to and rationalized in terms of microstructural differences characterized by OM and TEM. However, the extraordinary highest hardening behavior in A as envisaged in yield strength measurements after irradiation seems difficult to rationalize based only on the present results partly because of the limited capability of TEM in characterizing the responsibile irradiation- induced or enhanced damage microstructures. In this sense, further study using a wide array of advanced, sophistigated tools (for example, SANS, APFIM) are required to understand and fully characterize the irradiation hardening behavior of present RPV steels.. The highest hardening behavior of A suggests that the material-specific embrittlement prediction method that considers the differences in the unirradiated microstructural state may be developed and applied.

Acknowledgement

The authors acknowledge Drs. Jan Kocik and Anna Brozova, NRI, Czech for their help in performing TEM on irradiated RPV specimens. This study has been carried out under the nuclear R&D program(Korea-Czech joint research project) by MOST, Korea..

Reference

[1] W. A. Pavinich, Proceedings of the Second International Symposium on Environmental Degradation of Materials in Nuclear Power Systems-Water Reactors, Monterey, California Sept. 9-12, 1985, pp. 485-495.

[2] Se-Hwan Chi, Jun-Hwa Hong, and In-Sup Kim, Scripta Metallurgica et Materialia, 30 (1994) 1994.

[3] N. F. Panayotou, R. J. Puigh, and E. K. Opperman, J. Nucl. Mater., 103-104 (1981) 1523.

[4] Report on the KAERI Sample Irradiation, Nuclear Research Institute Rez plc, DIM-OMV97, Dec. 1997.

[5] G. R. Odette and G. E. Lucas, Final Report RP-1021-7, 1990, EPRI.

[6] J. T. Buswell, Examination of materials by electron microscopy. In Analsis of the Behavior of Advanced Reactor Pressure Vessel Steels Under Neutron Irradiation. The UK Programme UKAEA, 1983, 281.

[7] R. H. Sterne and L. E. Steele, Nucl. Eng. and Design, 10 (1969)259.

[8] Marshall Report/LWRSG(PV) 1982. p. 12.

[9] Minfa Lin, S. S. Hansen, T. D. Nelson, R. B. Focht, ASTM STP 1259, E. G. Nisbett and A. S. Melilli, Eds., ASTM, 1997 (in press).

[10] S. Ohtani, S. Okaguchi, Y. Fujishiro, and Y. Ohmori, Metall. Trans. A, 21A (1990) 877, and Private Communications with Y. R. Lim, Seoul National University.

[11] D. R. Olander, Fundamental Aspects of Nuclear Reactor Fuel Elements, TID-26711-P1, Technical Information Center, Energy Research and Development Administration, 1976. p. 431.

[12] Unpublished Results, KAERI (1997).

[13] Analysis of The Behavior of Advanced Reactor Prevessel Steels Under Neutron Irradiation, Technical Report Series No. 265, IAEA, Vienna, 1986. pp. 29-35.

[14] p. 29 in Ref. [13].

[15] p. 34 in Ref. [13].

[16] Se-Hwan Chi, G. E. Lucas, J. H. Hong, G. R. Odette, Differences in Mechanical Properties and Microstructure of SA 508 Cl. 3 Reactor Pressel Vessel Steels Manufactured by Different Steel Refining Process, *Submitted for publication in J. Nucl. Mater., 1998.*

[17] Recent Progress in Understanding Reactor Pressure Vessel Steel Embrittlement, In

Fundamentals of Radiation Damage and Challanges for Future Nuclear Materials, Ishino Conference, *The University of Tokyo*, Collected Abstracts, Dec. 15-16, 1994. pp.30 - 31.
[18] *Radiation Damage of Structural Materials*, Materials Science Monograph, 79., J. Koutsky and J. Kocik Eds. Elsevier Pub., 1994. p.70.
[19] p. 31 in Ref. [17].

Table 1. Chemical composition and steel refining process of SA 508 Cl. 3 steel A, B, C, and D which are differ in steel refining process.

Specimen I. D	SRP*	C	Si	Ni	Mn	Cr	Mo	Cu	P	N	Al
A	VCD	0.18	0.08	0.77	1.40	0.15	0.53	0.06	0.005	0.004	<20ppm
B	VCDA	0.17	0.10	0.82	1.35	0.16	0.50	0.03	0.006	55ppm	0.015
C	SA(I)	0.21	0.24	0.92	1.36	0.21	0.49	0.03	0.007	52 “	0.022
D	SA(II)	0.19	0.20	0.82	1.44	0.15	0.55	0.03	0.006	89 “	0.020

SRP*: Steel Refining Process, VCD:Vacuum Carbon Deoxidation,
VCDA:Vacuum Carbon Deoxidation plus Aluminum treatment,
SA(I) and SA(II): Silicon deoxidation plus Aluminum treatment in two different factory, I and II.

Table 2. Heat treatment condition of material A, B, C, and D.

Material	Heat Treatment Condition
A, B, C	Quenching: 650/690℃ (4 hr), 860～900℃ (6 hr) Water quenching to 60℃ Tempering: 650 ～ 670℃ (9～12 hr) Postweld Heat Treatment: 621±14 ℃ (30 hr)
D	Quenching: 870/897℃ (14.2 hr), water quenching Tempering: 650/663℃ (12.4 hr), air cooling Postweld Heat Treatment: 595/625℃ (14.4 hr), furnace cooling

Table 3. Grain size, carbide and precipitates morphology, and bainite lath structure obtained by optical microscope, and TEM on thin films and carbon replicas for A, B, C, and D steels.

Material	Grain Size		Precipitates, Carbide, and Bainite Morphology and Lath width(㎛)	Remarks
	ASTM	SIZE(㎛)		
A	7.6	22.3	Round(dia: ~0.5 ㎛), Fine Needle(50~100nm), Agglomerated, large and localized coarse carbides, Underdeveloped lath boundary, lath width: 5 ㎛. Coarse interlath carbide. PPts No: 6 x 10^7/mm^2 (Round:Needle=1:0.85)	
B	8.7	15.4	Round(dia:0.05~0.25 ㎛), Fine Needle(80 nm), Slightly agglomerated, Semi-underdeveloped lath boundary, lath width: 5 ㎛, Interlath carbide, PPts No.:8.5 x 10^6/mm^2 Round:Needle=1: 22	Incomplete replication
C	8.7	15.4	Round(dia: 0.025 ㎛, Needle(80nm), Square-like needle(100nm), Three types of carbides morphology, PPts at GB and matrix, Well developed lath boundary, lath width: 3.5 ㎛, Interlath carbides, PPts No.: 3.1 x 10^9/mm^2, Round:Needle:Square Needle = 1:1.75:0.46.	
D	9.5	12.5	Round(<0.05㎛), Needle(50~100nm), Fine round carbide, Well developed lath boundary, lath width: 2 ㎛, No interlath carbides, PPts No.:6.7 x 10^7/cm^2., Round:Needle=1:0.39.	

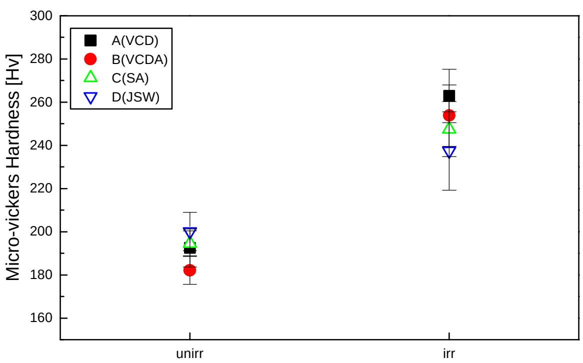

Fig. 3 Irradiation-induced change of Micro-vickers hardness of RPV low alloy steels A, B, C, and D(2.7 X 10^{19}n/cm^2, 288¡É).